Spin reversal effect in hybrid $s_{\pm}$-wave/p-wave Josephson junction

2010 J. Phys.: Condens. Matter 22 225701

(http://iopscience.iop.org/0953-8984/22/22/225701)

J. Phys.: Condens. Matter **22** (2010) 225701 (6pp) doi:10.1088/0953-8984/22/22/225701

Spin reversal effect in hybrid $s_{\pm}$-wave/p-wave Josephson junction

J Wang[1] **and K S Chan**[2]

[1] Department of Physics, Southeast University, Nanjing 210096, People's Republic of China
[2] Department of Physics and Materials Science, City University of Hong Kong, Tat Chee Avenue, Kowloon, Hong Kong, People's Republic of China

E-mail: junwang@nju.edu.cn and apkschan@cityu.edu.hk

Received 10 March 2010, in final form 9 April 2010
Published 20 May 2010
Online at stacks.iop.org/JPhysCM/22/225701

Abstract

We report a theoretical study on a hybrid Josephson junction consisting of a proposed $s_{\pm}$-wave ferropnictide superconductor and a p-wave superconductor. It is found that the relative π phase shift intrinsic to the $s_{\pm}$-wave pairing can lead to an accumulated spin reversal effect at the junction interface and that the critical current has a vanishing point with the variation of the ratio of the interface resistances for each band. The spin reversal effect also appears with an increase of temperature and meanwhile the critical current exhibits a reentrant behavior. These findings can not appear for a usual s-wave state, so that they can be used to discriminate the $s_{\pm}$-wave pairing in superconducting ferropnictides from the conventional s-wave symmetry.

(Some figures in this article are in colour only in the electronic version)

1. Introduction

Recently, the discovery of superconductivity in ferropnictides has triggered a surge of investigations in the research community and many research works were dedicated to this field [1–4]. For all the newly discovered superconductors (S), the principal task is to determine the order parameter symmetry of superconductivity. The ferropnictides have a complex band structure [5, 6], in which the Fermi surface consists of four sheets, two of which are hole-like and the other two are electron-like. All possible order parameter symmetries [7–9], such as s-wave, d-wave, and p-wave, have been proposed to account for its superconductivity; for example, the experiments on nuclear magnetic resonance [10, 11], the penetration depth [12, 13], and specific heat [14] revealed the signature of the nodes in the gap, whereas angular resolved photoemission spectroscopy [15] clearly showed the presence of the gap at all points on the Fermi surface.

At present there is no conclusive agreement on the order parameter symmetry of the ferropnictides S, but the so-called $s_{\pm}$ pairing symmetry [9, 16] is the leading contender, i.e., the Fermi surface is fully gapped and the gap functions for the electron and hole pockets have opposite signs. In order to distinguish it from the conventional s-wave pairing, many theoretic works were dedicated to studying its quantum transport properties [17–27]. For instance, the Andreev bound state (ABS) [17] at the material surface has been proposed to identify the $s_{\pm}$-wave pairing, since the reflected quasiparticle may feel the opposite sign of the S order parameter through the interband scattering, however, this ABS has its own drawback that it is energy-continuous and **k**-dependent and thus there is no outstanding peak in the density of states or the differential conductance in the energy gap. Moreover, the measurement based on the polycrystalline sample may smear the ABS effect due to its momentum dependence.

Other transport properties for $s_{\pm}$-wave pairing which have been studied include the multiband tunneling spectroscopy with the help of the BTK theory [18–20], and various Josephson effects in different junction structures [21–25]. Among these, the predicted 0–π transition [26, 27] in the s/$s_{\pm}$ junction seems attractive since its experimental measurement is straightforward and not limited to single crystal samples. The 0–π transition in the S/FM/S junction (FM: ferromagnetic metal) has been extensively studied [28] and its key mechanism is the tunneling Cooper pair in the FM region having a nonzero momentum due to the FM exchange splitting. The newly predicted 0–π transition [26, 27] in s/$s_{\pm}$ junction comes from the relative internal phase shift between the two bands in the $s_{\pm}$-wave S as well as the unequal interface resistance for the two bands; so one can modulate the transparency of the junction and even the temperature to realize the reversal of the critical current.

Recently, Sengupta *et al* [29] and Lu *et al* [30] have found that a spontaneous spin accumulation forms at the interface of the hybrid conventional s-wave/p-wave (s/p) Josephson junction and the spin polarization is along the **d** vector of the p-wave S. The physical origin is ascribed to the different spin pairing states and the orbital symmetries of the Cooper pairs. We notice that when an $s_{\pm}$-wave S and p-wave S constitute a Josephson junction ($s_{\pm}$/p), the spin accumulation will disappear or its direction can be reversed by modulating the interface resistances for the two bands of the $s_{\pm}$-wave S, while the spin reversal effect can be readily measured in experiments by the optical Kerr effect or an SQUID. Thus in this work, we study the spin accumulation at the interface of a hybrid $s_{\pm}$/p junction and consider the possible interband scattering effect using a minimal model. It is shown that the accumulated spin at the interface can be reversed by modulating the interface transparency and also by the temperature, the Josephson current exhibits a clear vanishing point with variation of the ratio of the interface resistances, and a reentrant behavior with temperature, which are solely explained by the relative phase shift between the two bands in the $s_{\pm}$-wave S. The phenomena found can not occur in a conventional s/p junction, so this hybrid junction can be used to discriminate the $s_{\pm}$-wave from the usual s-wave pairing. Moreover, the predicted spin reversal is qualitatively independent of the interband scattering strength.

The organization of this paper is as follows. In section 2, we present the theoretical model and the formulae for the calculation of spin density and supercurrent in a conventional s/p junction. In section 3, the $s_{\pm}$/p Josephson junction is studied with same method introduced in section 2. Finally, a brief conclusion is drawn in section 4.

2. s/p junction

In this section, we focus on the spin accumulation in a conventional s/p junction because, although the hybrid s/p junction [31] has been studied extensively, the spin accumulation is a new phenomenon found recently and to which little attention was been paid. Thus we first investigate it with a simplified model and then extend it to the $s_{\pm}$/p junction in next section. As schematically shown in figure 1, the s/p junction consists of a conventional s-wave S in the left lead, a p-wave S in the right lead, and an insulator barrier or normal metal between them; the z-axis set as the quantum spin axis is perpendicular to the junction interface and the **d** vector in the p-wave S is set along the x-axis. Since the **d** vector resembles an FM moment, but without destroying the time reversal symmetry of the system in the unitary case $\mathbf{d}\times\mathbf{d}^{*}=0$ considered here, the polarization of the possible spin density at the interface is solely determined by the **d** vector. The following mean field BCS Hamiltonian in a lattice version [32, 33] is employed here to describe the s/p junction

$$H = H_{\mathrm{L}} + H_{\mathrm{R}} + H_{\mathrm{T}}, \tag{1}$$

$$H_{\mathrm{L}} = \sum_{\mathbf{r}\langle\mathbf{a}\rangle} \tilde{C}^{\dagger}_{\mathbf{r}} h_0 \tilde{C}_{\mathbf{r}} + (\tilde{C}^{\dagger}_{\mathbf{r}} t_h \tilde{C}_{\mathbf{r}+\mathbf{a}} + \mathrm{c.c.}) + (\tilde{C}^{\dagger}_{\mathbf{r}} \Delta_{\mathrm{L}} \tilde{C}^{\dagger}_{\mathbf{r}} + \mathrm{c.c.}), \tag{2}$$

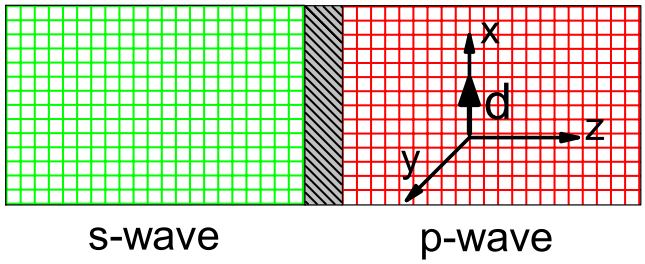

Figure 1. Schematic of the hybrid Josephson junction composed of the left s-wave S lead and right p-wave S lead. The gray region between two S leads is an insulator barrier or normal metal. The **d** vector in p-wave S is parallel to the x-axis and the current is flowing z-axis.

$$H_{\mathrm{R}} = \sum_{\mathbf{r}\langle\mathbf{a}\rangle} \tilde{C}^{\dagger}_{\mathbf{r}} h_0 \tilde{C}_{\mathbf{r}} + (\tilde{C}^{\dagger}_{\mathbf{r}} t_h \tilde{C}_{\mathbf{r}+\mathbf{a}} + \mathrm{c.c.}) + (\mathrm{i}\tilde{C}^{\dagger}_{\mathbf{r}} \Delta_{\mathrm{R}} \tilde{C}^{\dagger}_{\mathbf{r}+\mathbf{a}} + \mathrm{i}\tilde{C}_{\mathbf{r}} \Delta^{\dagger}_{\mathrm{R}} \tilde{C}_{\mathbf{r}+\mathbf{a}} + \mathrm{c.c.}), \tag{3}$$

$$H_{\mathrm{T}} = \tilde{C}^{\dagger}_{\mathrm{L}} h_t \tilde{C}_{\mathrm{R}} + \mathrm{c.c.}, \tag{4}$$

where $\tilde{C}_{\mathbf{r}} = (C_{\mathbf{r}\uparrow}, C_{\mathbf{r}\downarrow})^{\mathrm{T}}$, $h_0 = (2dt - \mu)\sigma_0$, $t_h = -t\sigma_0$, $\Delta_{\mathrm{L}} = \mathrm{i}\Delta_{\mathrm{s}}\sigma_y \mathrm{e}^{\mathrm{i}\phi_{\mathrm{L}}}$, $\Delta_{\mathrm{R}} = \mathrm{i}\Delta_{\mathrm{p}}\mathrm{e}^{\mathrm{i}\phi_{\mathrm{R}}}(\mathbf{d}\cdot\boldsymbol{\sigma})\sigma_y$, and $h_t = -t'\sigma_0$; σ_0 is a unit matrix, $\boldsymbol{\sigma}$ is the Pauli matrix, d is the dimension of the system, μ is the chemical potential, Δ_{s} and Δ_{p} are respectively the magnitudes of the order parameters of the s-wave and p-wave S leads, and $\phi_{\mathrm{L(R)}}$ is the macroscopic S phase of the left (right) S; $C^{\dagger}_{\mathbf{r},\sigma}$ ($C_{\mathbf{r},\sigma}$) is the creation (annihilation) operator of an electron at $\mathbf{r}$ with spin $\sigma =\uparrow,\downarrow$, the hopping integral t is considered between the nearest neighboring sites with a lattice vector $\mathbf{a}$. Both H_{L} and H_{R} are the mean field BCS Hamiltonians describing the left and the right S, respectively; H_{T} is the tunneling term connecting the left and right leads with t' the hopping integral, and $C^{\dagger}_{\mathrm{L(R)}\sigma}$ being the creation operator for the edge sites of the left (right) lead.

To obtain an analytic result, we study the 1D case of the s/p junction and the qualitative conclusions should remain unchanged in the 2D or 3D case with the summation over the transverse modes. With the help of the Keldysh Green function, the spin density $\mathbf{S}_{\mathrm{L}}$ and the supercurrent I_{L} in the left S lead are given by

$$\mathbf{S}_{\mathrm{L}} = \frac{\hbar}{2}\int \frac{\mathrm{d}E}{2\mathrm{i}\pi}\mathrm{Tr}[\boldsymbol{\sigma} G^{<}_{\mathrm{LL}}(E)], \tag{5}$$

and

$$I_{\mathrm{L}} = \frac{e}{\hbar}\int \frac{\mathrm{d}E}{2\pi}\mathrm{Tr}[h_{\mathrm{LR}} G^{<}_{\mathrm{RL}}(E) - G^{<}_{\mathrm{LR}}(E) h_{\mathrm{RL}}], \tag{6}$$

where $G^{<}_{\eta\sigma\eta'\sigma'}(t,t') = \mathrm{i}\langle C^{\dagger}_{\eta\sigma}(t) C_{\eta'\sigma'}(t')\rangle$ is the lesser Green function in the Nambu space and spin space, $h_{\eta\eta'} = -t'\sigma_z$ is the h_t in the Nambu space by assuming t' real, $\eta(\eta') = \mathrm{L}, \mathrm{R}$, and the trace is over the spin space. The spin density $\mathbf{S}_{\mathrm{L}}$ denotes the possible spin accumulation at the interfaces of the hybrid junction. Since the equilibrium case is considered and no bias is applied on the system, the equations above can be simplified by the Keldysh formula $G^{<}(E) = (G^{\mathrm{a}}(E) - G^{\mathrm{r}}(E))f(E)$, where $G^{\mathrm{r(a)}}$ is the retarded (advanced) Green function and

$f(E)$ is the Fermi distribution function. The retarded Green function can be worked out by the Dyson equation

$$G^{ra}_{\eta\eta} = [(g^{ra}_{\eta})^{-1} - \Sigma^{ra}_{\bar{\eta}}]^{-1}, \tag{7}$$

where $\Sigma^{r}_{\bar{\eta}} = h_{\eta\bar{\eta}} g^{r}_{\bar{\eta}} h^{\dagger}_{\eta\bar{\eta}}$ is the self-energy of the $\bar{\eta}$ ($\bar{\mathrm{L}}(\bar{\mathrm{R}}) = \mathrm{R(L)}$) lead, g^{r}_{η} is the surface Green function of the isolated S lead [34, 35],

$$g^{r}_{\mathrm{L}} = \begin{pmatrix} b_{\mathrm{L}}\sigma_0 & \mathrm{i}c_{\mathrm{L}}\sigma_y \mathrm{e}^{\mathrm{i}\phi_{\mathrm{L}}} \\ -\mathrm{i}c_{\mathrm{L}}\sigma_y \mathrm{e}^{-\mathrm{i}\phi_{\mathrm{L}}} & b_{\mathrm{L}}\sigma_0 \end{pmatrix} \tag{8}$$

and

$$g^{r}_{\mathrm{R}} = \begin{pmatrix} b_{\mathrm{R}}\sigma_0 & c_{\mathrm{R}}\sigma_z \mathrm{e}^{\mathrm{i}\phi_{\mathrm{R}}} \\ -c_{\mathrm{R}}\sigma_z \mathrm{e}^{-\mathrm{i}\phi_{\mathrm{R}}} & b_{\mathrm{R}}\sigma_0 \end{pmatrix}, \tag{9}$$

where $b_{\mathrm{L}} = -\mathrm{i}\pi\rho_{\mathrm{L}} E/\Omega_{\mathrm{L}}$, $b_{\mathrm{R}} = -\mathrm{i}\pi\rho_{\mathrm{R}}\Omega_{\mathrm{R}}/E$, $c_{\mathrm{L}} = -\mathrm{i}\pi\rho_{\mathrm{L}}\Delta_{\mathrm{s}}/\Omega_{\mathrm{L}}$, $c_{\mathrm{R}} = -\mathrm{i}\pi\rho_{\mathrm{R}}\Delta_{\mathrm{T}}/E$, $\Delta_{\mathrm{T}} = 2\sin(k_z a)\Delta_{\mathrm{p}}$ is assumed a positive constant in the following calculation, and here the p_z symmetry of the p-wave order parameter is considered so that $\Delta_{\mathrm{T}}(k_z) = -\Delta_{\mathrm{T}}(-k_z)$; $\Omega_{\mathrm{L(R)}} = \sqrt{E^2 - \Delta^2_{\mathrm{s(T)}}}$ as $E > -\Delta_{\mathrm{s(T)}}$ and $\Omega_{\mathrm{L(R)}} = -\sqrt{E^2 - \Delta^2_{\mathrm{s(T)}}}$ as $E < -\Delta_{\mathrm{s(T)}}$, $\rho_{\mathrm{L(R)}}$ is a constant density of states of the left (right) S lead at the Fermi energy. It is seen that for the left conventional s-wave S lead, the surface Green function is same as the bulk one and the right surface Green function has a singularity at $E = 0$, which is actually the zero energy edge state of the p-wave S lead with p_z symmetry considered. It is noted in an isolated single s-wave and p-wave S lead that the spin is degenerate and unpolarized, as is also seen in the equations above. The case is different when they are connected to each other, since in the spin space of the order parameter, the diagonal terms of the p-wave equal $\Delta_{\uparrow\uparrow} = \Delta_{\downarrow\downarrow} = \Delta_{\mathrm{T}}$ (equal spin pairing) while the s-wave is nonzero only in the off-diagonal term Δ_{s}, so that in the eigenspace of order parameter, the diagonal term can be different and is given by $\Delta_{\mathrm{T}} \pm \Delta_{\mathrm{s}}$, this can be clearly seen when the spin quantum axis is set along the **d** vector along the x-axis. Therefore, it is possible for a net spin density to form at the interface of the hybrid junction.

For comparison, the conductance of the normal junction without any S order parameter can be worked out by the Keldysh Green function

$$G = \frac{2e^2}{h}\frac{4t_0}{(1+t_0)^2} \tag{10}$$

with $t_0 = \pi^2\rho^2 t'^2$ denoting the interface transparency between the two leads, where two sides of the junction are assumed identical $\rho_{\mathrm{L}} = \rho_{\mathrm{R}} = \rho$; as $t_0 = 1$, the conductance of the junction is at the resonant point $G_0 = 2e^2/h$, which means the interface is fully transparent. With direct algebra, the supercurrent in left lead reads ($\phi = \phi_{\mathrm{R}} - \phi_{\mathrm{L}}$)

$$I_{\mathrm{L}} = \frac{8e}{h}\int \mathrm{d}E\, f(E) \times \mathrm{Im}\left[\frac{\Delta_0^4 t_0^2 \sin(2\phi)}{(E^4 - E^2\Delta_0^2)(1+t_0)^4 + 2t_0^2\Delta_0^4(1-\cos(\phi))}\right]. \tag{11}$$

Here we have assumed $\Delta_{\mathrm{s}} = \Delta_{\mathrm{T}} = \Delta_0$ for simplicity so that the two S leads are same except for the order parameter symmetries and the S macroscopic phases, the supercurrent is proportional to $\sin 2\phi$ unlike the usual $\sin\phi$ in the conventional s/s junction, which is a typical characteristic of the s/p junction due to the orthogonality of the orbital wavefunctions between s-wave and p-wave Cooper pairs [31]. As shown in figure 2(a), the oscillating period of the supercurrent is π, therefore, it is expected the current direction should remain unchanged when there is a π phase shift between the two bands in the $\mathrm{s}_{\pm}$-wave S, but it does not mean the current in the $\mathrm{s}_{\pm}$/p junction is entirely the same as that in the s/p junction; on the contrary, the supercurrent in the $\mathrm{s}_{\pm}$/p junction may exhibit a distinctive zero due to the quantum coherent transport. With different interface transparency $t_0 = 1$, and 0.5, the results remain almost unchanged in figure 2(a), this is attributed to the edge state in the p-wave S lead since the p_z symmetry of the order parameter is considered. The spin density in the left S surface is given by

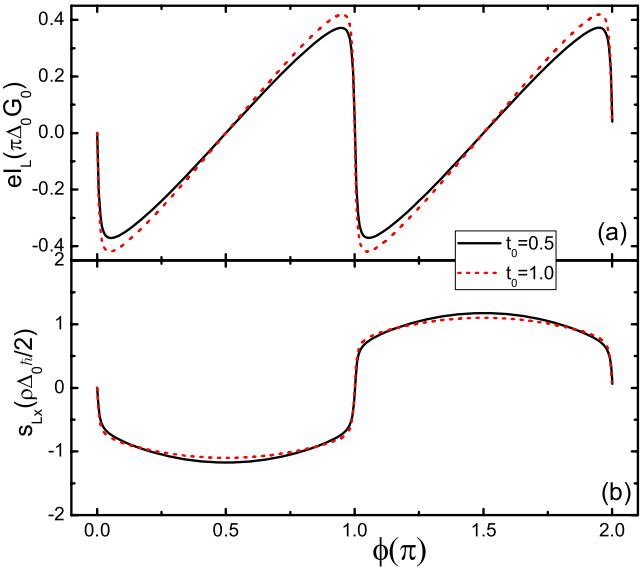

Figure 2. The supercurrent I_{L} (a) and spin density $S_{\mathrm{L}x}$ (b) as a function of the macroscopic phase difference ϕ for different interface transparencies $t_0 = 1.0$ and $t_0 = 0.5$. $\Delta_0 = 1$ is taken as the energy unit and temperature $T = 0$.

$$S_{\mathrm{L}x} = \int \mathrm{d}E\, f(E) \times \mathrm{Im}\left[\frac{2\hbar\rho\Delta_0^2 t_0[E^2(1+t_0) - t_0\Delta_0^2]\sin\phi}{(-E^4 + E^2\Delta_0^2)(1+t_0)^4 - 2t_0^2\Delta_0^4(1-\cos(\phi))}\right], \tag{12}$$

$$S_{\mathrm{L}y} = 0, \tag{13}$$

$$S_{\mathrm{L}z} = 0. \tag{14}$$

Here only $S_{\mathrm{L}x}$ is nonzero, it can be understood that the symmetry of the **d** vector of the p-wave in spin space is broken due to the introduction of the spin singlet order parameter of the s-wave, and subsequently the polarization of the spin accumulation (imbalance) is along the **d** vector (x-axis) [29, 30]. The spin density in the right surface $\mathbf{S}_{\mathrm{R}}$ has the same tendency and is not shown again here. As shown in figure 2(b), the spin density is an odd function over the S phase

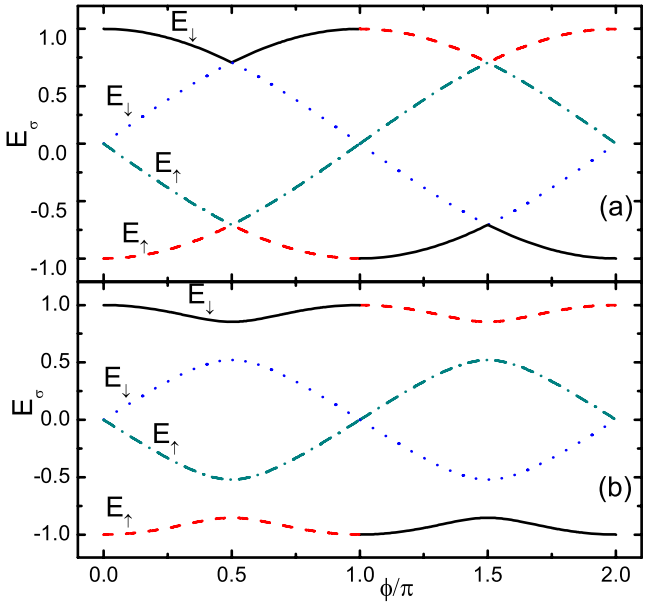

Figure 3. The ABS energy versus the phase ϕ, $\Delta_0 = 1$, the temperature $T = 0$; $\sigma = \uparrow, \downarrow$ is parallel to the **d** vector, (a) $t_0 = 1.0$, (b) $t_0 = 0.5$.

difference ϕ, and the spin direction can be reversed when there is a π phase shift in ϕ. Similarly, the spin accumulation is again not sensitive to the interface transparency due to the edge state.

To discern clearly the spin accumulation, we can obtain the ABS energy from the poles of Green's function $G^{\mathrm{r}}_{\mathrm{LL}}$ in equation (7) or the poles of the integral of equation (12), it is written as

$$E^2 = \Delta_0^2 \left(\frac{1 \pm \sqrt{1-c}}{2} \right) \tag{15}$$

with $c = 8t_0^2(1 - \cos(2\phi))/(1 + t_0)^4$. The expression is relatively succinct since equal magnitudes of pair potentials in the two S leads are assumed. As shown in figure 3, it is spin split so that the different spin species locate oppositely at $E > 0$ or $E < 0$, which are the same as those obtained from a scattering method in [29]. From equation (8), the spin space is degenerate in the s-wave S whereas in the p-wave S the spin-up space has π phase shift in ϕ_{R} over the spin-down space, so that the ABS has a relation $E_\sigma(\phi) = E_{-\sigma}(\pi + \phi)$. Different from the conventional s/s junction, the ground state of the s/p Josephson junction has $\phi = \pm\pi/2$, and meanwhile there is no supercurrent flowing in the junction, a spin accumulation can therefore spontaneously occur at the interface of the hybrid junction with either $\phi = \pi/2$ or $3\pi/2$, as shown in figure 2.

3. $s_\pm$/p junction

In section 2, we have shown a spontaneous spin accumulation at the interface of the s/p junction due to the broken symmetry of the **d** vector in the spin space, and the spin polarization is parallel to the **d** vector, moreover, the accumulated spin density is an odd function of the S phase difference ϕ with period 2π. Thus, when the $s_\pm$/p junction is taken into account, it is possible to realize the spin reversal effect by modulating some system parameters, such as the interface transparency and the temperature. We adopt a minimal model below to mimic the $s_\pm$-wave S while its pairing mechanism or the origin of π phase shift is not our concern here. The Hamiltonian of the hybrid $s_\pm$/p junction is now given by

$$H = H_{\mathrm{L1}} + H_{\mathrm{L2}} + H_{\mathrm{R}} + H_{\mathrm{T1}} + H_{\mathrm{T2}} + H_{\mathrm{T12}}, \tag{16}$$

where H_{L1} and H_{L2} are the same as H_{L} in equation (2) describing the two bands in the left $s_\pm$-wave S with a sign reversal in their order parameters; H_{R} keeps unchanged as equation (3); H_{T1} and H_{T2} are the coupling between the two bands in the $s_\pm$-wave and p-wave S leads, respectively; while H_{T12} describes the interband scattering in the $s_\pm$-wave S at the interface of junction [27]. As with the hopping element t' in equation (4), t_1, t_2, and t_{12} represent the corresponding hopping constants between H_{L1} and H_{R}, H_{L2} and H_{R}, and H_{L1} and H_{L2}, respectively. The calculations of the Josephson current and spin density are still based on equations (5) and (6), where the difference is that we need to sum over the two bands in the $s_\pm$-wave S lead like the two transport channels considered. As stated above, the important step to work out I_{L} and $S_{\mathrm{L}x}$ is to determine the retarded Green function $G^{\mathrm{r}}_{\eta\eta'}$; it is convenient for our model to use the following Dyson equation to work out the coupled Green functions

$$G^{\mathrm{r(a)}} = G_0^{\mathrm{r(a)}} + G^{\mathrm{r(a)}} V G_0^{\mathrm{r(a)}} \tag{17}$$

with

$$G_0^{\mathrm{r}} = \begin{pmatrix} g^{\mathrm{r}}_{\mathrm{L1}} & 0 & 0 \\ 0 & g^{\mathrm{r}}_{\mathrm{L2}} & 0 \\ 0 & 0 & g^{\mathrm{r}}_{\mathrm{R}} \end{pmatrix} \tag{18}$$

and

$$V = \begin{pmatrix} 0 & h_{\mathrm{L1,L2}} & h_{\mathrm{L1,R}} \\ h^\dagger_{\mathrm{L1,L2}} & 0 & h_{\mathrm{L2,R}} \\ h^\dagger_{\mathrm{L1,R}} & h^\dagger_{\mathrm{L2,R}} & 0 \end{pmatrix}, \tag{19}$$

where $g^{\mathrm{r}}_{\mathrm{L1}}$, $g^{\mathrm{r}}_{\mathrm{L2}}$ are the surface Green functions of the two bands in the $s_\pm$-wave S lead, $g^{\mathrm{r}}_{\mathrm{R}}$ is the one of the p-wave lead, which are explicitly given in equations (8) and (9), $h_{\eta,\eta'}$ ($\eta = \mathrm{L1}, \mathrm{L2}, \mathrm{R}$) is the coupling matrix between different bands in the Nambu and spin space.

Since the analytic expressions for I_{L} and $S_{\mathrm{L}x}$ are too long, we only present the numerical results in figures 4 and 5. The different coupling constants t_1, t_2, and t_{12} in our model can actually account for the mismatch factors among different bands in both the $s_\pm$ and p-wave S, such as the Fermi wavevector mismatch; we therefore assume an equal density of states $\rho_{\mathrm{L1}} = \rho_{\mathrm{L2}} = \rho_{\mathrm{R}} = \rho$ in all bands as in the s/p case discussed above. In figure 4, the spin density and supercurrent are presented as a function of the ratio of t_1/t_2 with different interband couplings t_{12}. It is clearly shown that the direction of the accumulated spin is reversed as $t_1/t_2 = 1$, and meanwhile at the same point, the supercurrent exhibits a vanishing point.

The obtained results can be understood as follows: since the spin density $S_{\mathrm{L}x}$ formed at the interface of the s/p junction has the relation $S_{\mathrm{L}x}(\phi) = -S_{\mathrm{L}x}(\phi + \pi)$ (figure 2(b)), and in the $s_\pm$/p junction there exists a relative phase shift π between the two bands in the $s_\pm$-wave pairing state, so that the two

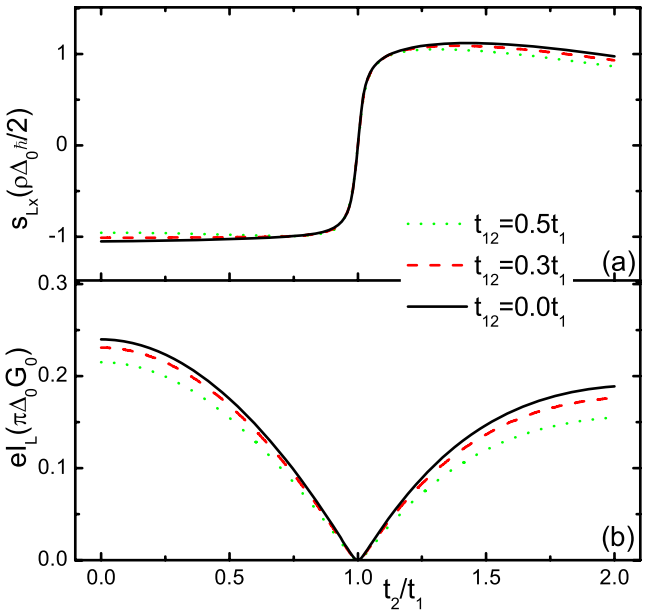

Figure 4. The dependence of I_L (a) and S_{Lx} (b) on the ratio of interface transparencies t_2/t_1 with different interband scattering, $t_{12} = 0$, $t_{12} = 0.3t_1$, $t_{12} = 0.5t_1$, $t_0 = 0.5$, $\phi = \pi/4$.

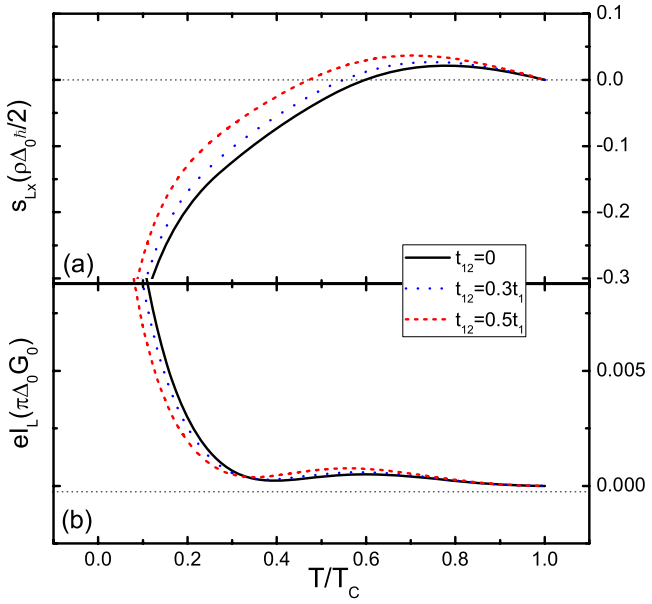

Figure 5. The temperature dependence of S_{Lx} (a) and I_L (b) with different interband scattering, $t_{12} = 0t_1$, $t_{12} = 0.3t_1$, $t_{12} = 0.5t_1$, $t_1/t_2 = 0.8$, other parameters are same as those in figure 4.

contributions to the accumulated spin have opposite signs, and at the same interface transparency $t_1 = t_2$ for the two bands, the spin accumulation vanishes entirely. The interband scattering t_{12} in the $s_\pm$-wave S does not result in a qualitative change of the I_L and S_{Lx} in figure 4, although this interband scattering is the key point for the ABS state formed at the surface of the $s_\pm$-wave S [17]. The spin reversal phenomenon does not occur in a single s/p junction on varying the interface resistance, and so it can be used to distinguish the $s_\pm$-wave pairing from the usual s-wave pairing state. The key point is to vary the interface transparency t_1 and t_2 for the two bands of the $s_\pm$-wave S, which is possible in experiment since there are several factors affecting the t_1 and t_2, such as the Fermi wavevector of each band, the density of states at the Fermi energy, and the different effective mass of the quasiparticles. As the two bands in $s_\pm$-wave are not exactly identical, one can modulate the relative magnitude t_1 and t_2 even by the barrier strength between two S leads. In figure 4(b), the supercurrent also exhibits a clear zero point at $t_1 = t_2$, which is again almost independent of the interband scattering t_{12}. Obviously, this zero point comes from the relative π phase shift for the two bands in the $s_\pm$-wave S, however, it is essentially different from the 0–π transition of the critical current in the $s_\pm$/s junction studied in [26]. Here the critical current in the $s_\pm$/p junction does not change its sign because the oscillating period of I_L is π and the π phase shift can not reverse the current direction. It is the coherent transport considered here that leads to the appearance of the vanishing of I_L.

As the 0–π transition in the $s_\pm$/s junction was predicted to be realized by modulating temperature [26], the spin reversal effect in the $s_\pm$/p junction may also appear on varying the temperature, it can facilitate greatly the experiment measurement in contrast to qualitative variation of the Fermi wavevector mismatch. Here it is assumed that the gaps in the two S leads have a BCS temperature dependence with the same critical temperature T_C but with a different gap magnitude. In figure 5, we present the dependence of the spin density and supercurrent on temperature for different interband scattering parameter t_{12}. As seen, the spin direction can be reversed with an increase of temperature for some suitable parameters and furthermore the supercurrent exhibits an reentrant behavior with temperature. The physics origin is the same as that explained above, it is the intrinsic phase shift for the two order parameters as well as the different gap magnitudes for the two bands in the $s_\pm$-wave S, where $\Delta_1 = 1.5\Delta_2 = \Delta_0$ are taken in calculations. This in physical terms the same as the 0–π transition predicted in the $s_\pm$/s junction from modulating temperature. The interband scattering is also considered and makes little difference to the supercurrent, while it can slightly change the transition temperature at which the spin is reversed, as shown in figure 5(a). Therefore, it is suggested that the presence the reentrant behavior of the critical current and the spin reversal phenomena should rule out the usual s-wave state.

4. Conclusion

In conclusion, we have investigated the supercurrent properties and spin reversal effect in the $s_\pm$/p hybrid junction. In a simplified model, we have shown that the relative π phase shift for the two order parameters in the $s_\pm$-wave S can lead to an accumulated spin reversal effect at the interface of the junction, the supercurrent has a clear vanishing point on varying the relative interface resistances for the two bands of the $s_\pm$-wave S, moreover, a spin reversal effect and reentrant behavior of the supercurrent can appear on modulating the temperature, which obviously facilitates the experimental observations. The interband scattering between the two bands in the $s_\pm$ lead was shown as not being crucial for the obtained results.

Our findings may be helpful for identifying the possible existence of an $s_{\pm}$-wave pairing state in the superconducting ferropnictides.

Acknowledgments

The work was supported by the General Research Fund of the Research Grants Council of Hong Kong SAR, China (Project No. CityU 100310/10P); JW thanks support from NSFC (10704016) and the National Basic Research Project of China (2009CB929504).

References

[1] Kamihara Y, Watanabe T, Hirano M and Hosono H 2008 *J. Am. Chem. Soc.* **130** 3296
[2] Rotter M, Tegel M and Johrendt D 2008 *Phys. Rev. Lett.* **101** 107006
[3] Tapp J H, Tang Z, Lv B, Sasmal K, Lorenz B, Chu P W and Guloy A M 2008 *Phys. Rev.* B **78** 060505(R)
[4] Mazin L and Schmalian J 2009 arXiv:0901.4790 [cond-mat]
Boeri L, Dolgov O and Golubov A 2009 arXiv:0902.0288 [cond-mat]
[5] Singh D J and Du M H 2008 *Phys. Rev. Lett.* **100** 237003
[6] Kuroki K, Onari S, Arita R, Usui H, Tanaka Y, Kontani H and Aoki H 2008 *Phys. Rev. Lett.* **101** 087004
[7] Mazin I I, Singh D J, Johannes M D and Du M H 2008 *Phys. Rev. Lett.* **101** 057003
Cvetkovis V and Tesanovic Z 2009 *Europhys. Lett.* **85** 37002
[8] Lee P A and Wen X G 2008 *Phys. Rev.* B **78** 144517
[9] Chubukov A V, Efremov D V and Eremin I 2008 *Phys. Rev.* B **78** 134512
[10] Grafe H-J *et al* 2008 *Phys. Rev. Lett.* **101** 047003
[11] Nakai Y, Ishida K, Kamihara Y, Hirano M and Hosono H 2008 *J. Phys. Soc. Japan* **77** 073701
[12] Luetkens H *et al* 2008 *Phys. Rev. Lett.* **101** 097009
[13] Kofu M, Lee S-H, Fujita M, Kang H-J, Eisaki H and Yamada K 2009 *Phys. Rev. Lett.* **102** 047001
[14] Gordon R T *et al* 2009 *Phys. Rev. Lett.* **102** 127004
[15] Kondo T *et al* 2008 *Phys. Rev. Lett.* **101** 147003
[16] Wang F, Zhai H, Ran Y, Vishwanath A and Lee D-H 2009 *Phys. Rev. Lett.* **102** 047005
[17] Ghaemi P, Wang F and Vishwanath A 2009 *Phys. Rev. Lett.* **102** 157002
[18] Wang D, Wan Y and Wang Q-H 2009 *Phys. Rev. Lett.* **102** 197004
[19] Nagai Y and Hayashi N 2009 *Phys. Rev.* B **79** 224508
[20] Feng X-Y and Ng T-K 2009 *Phys. Rev.* B **79** 184503
[21] Ota Y, Machida M, Koyama T and Matsumoto H 2009 *Phys. Rev. Lett.* **102** 237003
[22] Ota Y, Machida M and Koyama T 2009 arXiv:0907.0277 [cond-mat]
[23] Wu J and Phillips P 2009 *Phys. Rev.* B **79** 092502
[24] Parker D and Mazin I I 2009 *Phys. Rev. Lett.* **102** 227007
[25] Tsai W-F, Yao D-X, Bernevig B A and Hu J 2008 arXiv:0812.0661 [cond-mat]
[26] Linder J, Sperstad I B and Sudbø A 2009 *Phys. Rev.* B **80** 020503(R)
[27] Sperstad I B, Linder J and Sudbø A 2009 arXiv:0908.1384 [cond-mat]
[28] Golubov A A, Kupriyanov M Yu and Il'ichev E 2004 *Rev. Mod. Phys.* **76** 411
Bergeret F S, Volkov A F and Efetov K B 2005 *Rev. Mod. Phys.* **77** 1321
Buzdin A I 2005 *Rev. Mod. Phys.* **77** 935
[29] Sengupta K and Yakovenko V M 2008 *Phys. Rev. Lett.* **101** 187003
[30] Lu C-K and Yip S 2009 *Phys. Rev.* B **80** 024504
[31] Asano Y 2005 *Phys. Rev.* B **72** 092508
Asano Y 2006 *Phys. Rev.* B **74** 220501(R)
[32] Cuevas J C, Martin-Rodero A and Levy Yeyati A 1996 *Phys. Rev.* B **54** 7366
[33] Asano Y, Tanaka Y and Kashiwaya S 2006 *Phys. Rev. Lett.* **96** 097007
[34] Aono T, Golub A and Avishai Y 2003 *Phys. Rev.* B **68** 045312
[35] Samanta M P and Datta S 1998 *Phys. Rev.* B **57** 10972